Combining algorithms for automatic detection of optic disc and macula in fundus images

Rashid Jalal Qureshi[1], Laszlo Kovacs[2], Balazs Harangi[3], Brigitta Nagy[4], Tunde Peto[5], Andras Hajdu[6]

[1,2,3,4,6]Faculty of Informatics, University of Debrecen, POB 12, 4010 Debrecen, Hungary
{rashid.jalal, kovacs.laszlo.ipgd, harangi.balazs, nagy.brigitta, hajdu.andras}@inf.unideb.hu
[5]NIHR Biomedical Research Centre for Ophthalmology, at Moorfields Eye Hospital NHS Foundation Trust and UCL Institute of Ophthalmology, 162 City Road, London, EC1V 2PD, UK
tunde.peto@moorfields.nhs.uk

Abstract—**This paper proposes an efficient combination of algorithms for the automated localization of the optic disc and macula in retinal fundus images. There is in fact no reason to assume that a single algorithm would be optimal. An ensemble of algorithms based on different principles can be more accurate than any of its individual members if the individual algorithms are doing better than random guessing. We aim to obtain an improved optic disc and macula detector by combining the prediction of multiple algorithms, benefiting from their strength and compensating their weaknesses. The location with maximum number of detectors' outputs is formally the hotspot and is used to find the optic disc or macula center. An assessment of the performance of integrated system and detectors working separately is also presented. Our proposed combination of detectors achieved overall highest performance in detecting optic disc and fovea closest to the manually center chosen by the retinal specialist.**

***Index Terms*— Diabetic retinopathy, macula detection, optic disc detection, retinal imaging**

I. INTRODUCTION

The retina is a delicate light sensitive lining located at the back of our eye that "takes pictures" and sends the images to the brain. Diabetic retinopathy (DR) is the damage to the eye's retina that occurs with long-term diabetes, which can eventually lead to blindness. The blood vessels that provide nourishment to the retina, in case of a person with diabetes may weaken and leak, forming small, dot-like hemorrhages. These leaking vessels often lead to swelling or edema in the retina and decreased vision. The fluorescein angiography and retinal photography are the most commonly used imaging of eye that provides ophthalmologists the possibilities to monitor the progression of the disease and to make decisions for the appropriate treatment. Screening programs for DR are being introduced and automation of image grading would have a number of benefits. However, an important prerequisite for automation is the accurate location of the main anatomical features in the image, notably the optic disc (OD) and the macula. The optic disc is a circular shaped anatomical structure with a bright appearance. It is the location where the optic nerve enters the eye. If the position and the radius of the optic disk are detected correctly, then they can be used as references for approximating other anatomical parts e.g. macula and the fovea. The macula is located roughly in the center of the retina, temporal to the optic nerve. It is a small and highly sensitive part of the retina responsible for detailed central vision. The macula allows us to appreciate details and perform tasks that require central vision such as reading. The fovea is the very center of the macula, the site of our sharpest vision (see Fig 1). Information about the locations of these features is necessary because the severity and characterization of abnormalities in the eye partially depends on their distances to the fovea. Optic disc detection is important in the computer-aided analysis of retinal images. It is crucial for the precise identification of the macula to enable successful grading of macular pathology such as diabetic maculopathy (clinically significant macular edema, macular ischemia). Much work has been carried out in this field and series of interesting algorithms includes [1-5] have been proposed in the recent past using various methods ranging from filtering [6] and threshold methods [7] to kNN regression [8]. Performance is generally good, but each method has situations, where it fails.

However, there is in fact no reason to assume that a single algorithm would be optimal for the detection of various anatomical parts of the retina. It is difficult to determine which one is the best approach because good results were reported for healthy retinas but less precise on a difficult data set i.e., the diseased retinas with variable appearance of ODs in term of intensity, color, contour definition etc.

In this paper, we suggest an approach to automatically combine different optic disc and macula detectors, to benefit from their strengths while overcoming their weaknesses. In particular, we propose a "flexible" (instead of

fixed) combination scheme which is triggered by hotspots - the region with maximum number of algorithms' outputs. In order to balance the contribution of individual algorithms participating in determining the final decision, weights are assigned to the outputs. The criterion for the selection of the candidate algorithms to be combined is based on different principles, good detection accuracy or low computation time. Experimental results and analysis are provided on the following three publically available databases Diaretdb0 [9], Diaretdb1 [10] and DRIVE [11]. We show that our combination approach outperforms the individual algorithms for both the detection of optic disc and the localization of the fovea.

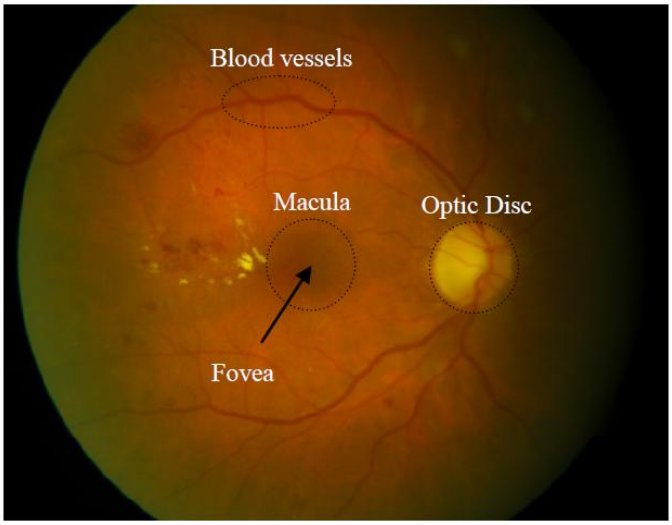

Fig. 1. A retinal fundus images and main anatomical features.

In the rest of the paper, section 2 presents some existing optic disc and macula detection algorithms which we have used in our proposed system. Section 3 motivates the use of ensemble methods as proposed procedure, while section 4 discusses the results. Section 5 gives conclusion and further recommendations.

II. Algorithms used for the proposed Ensemble-Based System

An ensemble of classifiers is a set of classifiers whose individual decisions are combined in some way (typically by unweighted or weighted voting) to classify new examples. The main discovery is that ensembles are often much more accurate than the individual classifiers that make them up. Imagine that we have an ensemble of three classifiers: $\{h_1, h_2, h_3\}$ and consider a new case $\mathbf{x}$. If the three classifiers are identical (i.e., not diverse), then when $h_1(\mathbf{x})$ is wrong, $h_2(\mathbf{x})$ and $h_3(\mathbf{x})$ will also be wrong. However, if the error made by the classifiers are uncorrelated, then when $h_1(\mathbf{x})$ is wrong, $h_2(\mathbf{x})$ and $h_3(\mathbf{x})$ may be correct, so the majority voting will correctly classify $\mathbf{x}$ [12]. Following this idea, we have collected a set of optic disc and macula detectors to benefit from their predictions for finding a more accurate optic disc and macula center.

2.1 Description of algorithms used for detecting optic disc

Although numerous optic disc algorithms have been developed, a major concern in constructing ensembles is how to select appropriate algorithms as ensemble components. A challenge is that there is not a single algorithm that can outperform any other algorithms in all respect i.e., to reduce the complexity and computational time while achieving better performance. Despite of these facts, we propose adopting the following OD detectors found to achieve better predictive accuracy when combined; nevertheless much effort has been devoted to this area and need further attention as well. We now discuss the key OD detector algorithms that have been improved and implemented.

2.1.1 Based on pyramidal decomposition (OD_{pd})

This algorithm relies on three assumptions. First, the image is centered on the macula or optic disc, second, the OD represents a bright region (not necessarily the brightest) and finally, the form of the OD is approximately circular. Based on the hypothesis that the optic disc is roughly a circular patch of bright pixels surrounded by darker pixels

Lalonde *et al*. [3] propose to locate the candidate OD regions on the green plane of the original image by mean of pyramidal decomposition (Haar-based discrete wavelet transform). In the low resolution image pixels which have the highest intensity values compared to the mean pixel intensity over the search area were selected as possible candidates. Next, smoothing is done within each of these regions and the brightest pixel is selected as a possible OD center point and its confidence value is computed as the ratio of average pixel intensity inside a circular region centered at the brightest pixel and the average intensity in its neighborhood.

2.1.2 Based on edge detection (OD_{ed})

In this method, Lalonde *et al*. [3] search the area identified by the pyramidal decomposition (see section 2.1.1) for a circular shape. To reduce the number of regions of interest, contiguous regions were aggregated into a single zone. A binary edge map is obtained by performing Canny edge detection in the region of interest first, and then a thresholded image I_T is obtained with a special threshold value computed from noisy edge map. The search for the OD contour is performed using an algorithm based on Hausdorff distance. The Hausdorff distance provide a degree of mismatch between two sets of points, defined as

$$H(A, B) = \max(h(A, B), h(B, A)) \text{ with}$$

$$h(A,B) = \max_{a \in A} \min_{b \in B} \|a - b\| .$$

Several circular templates of variable sized diameters were used to compute the Hausdorff distance between the templates and thresholded image I_T containing edges. Hence, a percentage of matches are computed, and if the certain proportion of the pixels template is found to overlap edge pixels in I_T then the location is retained as the centre point of a potential OD candidate.

2.1.3 Based on entropy filter (OD_{ef})

Sopharak *et al*. [4] presented the idea of detecting the optic disc by entropy filtering. The original RGB image is transformed into HSI color space, median filtering is applied to remove possible noise and for contrast enhancement contrast limited adaptive histogram equalization (CLAHE) is done to the I band. After preprocessing, optic disc detection is performed by probability filtering, using the following equation:

$$H(I_x) = -\sum_{i=0}^{255} P_{I_x}(i).\log P_{I_x}(i)$$

where P_{I_x} is the probability mass function of the pixel intensities I_x in a local neighborhood of x. Binarization is done with Otsu's algorithm [13] to separate the complex regions from the smooth ones, and the largest connected region with an approximately circular shape is marked as a candidate for the optic disc.

2.1.4 Based on Hough transformation (OD_{ht})

Ravishankar *et al.* [14] tried to track the optic disc by combining the convergence of the only thicker blood vessel initiating from it and high disk intensity properties in a cost function. On initially resized image to standard resolution (768 × 576), a grayscale closing operation is performed on the green channel image. This step is followed by thresholding and median filtering to obtain the binary image of the blood vessels. The segments of the thicker blood vessels skeleton are modeled as lines found by the Hough transform. The dataset of lines generated is reduced by removing those lines with slopes $\theta < 45^0$. This reduced dataset of lines is intersected pair- wise to generate an intersection map. The map is dilated to make the region of convergence more apparent. A weighted image is produced by combining this dilated intersection map and preprocessed green channel image. A cost function is defined to obtain the optimal location of the OD that is a point which maximizes the cost function.

2.1.5 Based on feature vector and uniform sample grid (OD_{fv})

Niemeijer *et al.* [15] defines a set of features based on vessel map and image intensity, like number of vessels, average width of vessels, standard deviation, orientation, maximum width, density, average image intensity etc., measured under and around a circular template to determine the location of the optic disc. After pre-processing, each image is scaled so that the width of its field of view (FOV) is 630 pixels. The binary vessel map obtained [16] is thinned until only the centerlines of the vessels remain and all the centerline pixels that have two or more neighbors are removed. Next, the orientation of the vessels is measured by applying principal component analysis on each centerline pixel with its neighboring pixel on both sides. A two step sampling process is launched to get the training database. First, using the circular template of radius r = 40 pixels having manually selected OD center within the radius, all features are extracted for each sample location (a uniform grid spaced 8 pixels apart) of the template including distance d to the true center. In the second step, 500 randomly selected location (i.e., not on a grid) in the training image were sampled in a similar fashion. To locate the OD, a sample grid (grid points spaced 10 pixels apart) is overlaid on top of the complete FOV and features vector are extracted and rough location of OD is found containing pixels having lowest value of d. The process is repeated with a 5x5 pixel grid centered on the rough OD location to get the more accurate OD center.

2 .2 Description of algorithms used for detecting macula

In this section, we present an overview of those macula detector algorithms that were selected for the ensemble-based system.

2.2.1 Macula detection based on intensity (M_I)

In [17] a region of interest (ROI) is defined to process macula detection. A Gaussian low pass filter is applied to smooth the intensity of the image. The statistical mean and standard deviation of the ROI area is used to compute a threshold for segmentation to get binary objects. The object that is located nearest to the center of the ROI is labeled as macula of the retina. Its center of mass is considered to be the center of the macula. However, we did some modification to this approach, because it is not mentioned in the article how this ROI is defined; therefore instead of restricting the process to a specific ROI we applied it to the whole image. The smoothing of the image is done using a large kernel (70 × 70 pixels with $\sigma = 10$) so that vascular network and small patches do not interfere in detection. Then, the thresholding based segmentation process is launched which generate a set of binary images corresponding to different threshold values in iteration. In each binary image, the object satisfying the area and distance from the center constraints are identified. Finally, the object found nearest to the center with minimum surface area is marked as macula

2.2.2 Macula detection based on spatial relationship with the optic disc (M_{sr})

In [18] a region of interest (ROI) for macula is defined by means of its spatial relationship with the optic disk. That is the portion of a sector subtended at the center of the optic disk by an angle of 30º above and below the line between this center and the center of the retinal image disk. The macula is identified within this ROI by iteratively applying a threshold, and then applying morphological opening (erosion followed by dilation) on the resulting blob. The value of the threshold is selected such that the area of the smoothed macula region is not more than 80% of that of the detected optic disk. The fovea is simply determined as the centroid of this blob.

2.2.3 Macula detection based on temporal arcade (M_{ta})

Fleming *et al.* [19] proposed to identify the macular region based on the information of the temporal arcade and optic disc center. First, the arcade was found by using semielliptical templates having a range of sizes, orientations, and eccentricities and having right- and left-handed forms. Next, the optic disc was detected by using a Hough transform with circular templates having diameters from 0.7 to 1.25 OD diameter (DD). Finally, the fovea was detected by finding the maximum correlation coefficient between the image and a foveal model. The search was restricted to a circular region with diameter 1.6 DD centered on a point that is 2.4 DD from the optic disc and on a line between the detected optic disc and the center of the semi-ellipse fitted to the temporal arcades.

2.2.4 Macula detection based on Watershed and morphological operators (M_{wm})

Zana *et al.* [20] presented a region merging algorithm based on watershed cell decomposition and on morphological treatments for macula recognition. After noise removal, morphological closing followed by opening is performed to remove the small dark holes and white spots. A watershed based decomposition of the gradient image into cells is done, and the cell with darkest gray level inside the macula is selected as the first step of a merging algorithm. A complex criterion based on the gray values and of edges of the filtered image is calculated to merge the cells of the macula while rejecting perifoveal inter-capillary zones in order to produce the contour of the macula.

2.2.5 A novel approach (M_n)

Besides the algorithms discussed so far, we have also tested our novel contribution for macula detection and used its results in our combined system. First, we extract the green plane form the color fundus image. Then, we generate the background image by applying an $A \times A$ median filter and subtract it from the green plane, resulting in a shade corrected image. Next, we binarize the image by considering all-non zero pixels as foreground pixels, and others as background. Finally, we apply an image labeling procedure and select the largest component as the macula.

III. PROPOSED COMBINATION OF THE ALGORITHMS

As discussed in [12], an ensemble classifier can be more accurate than any of its individual members if the individual classifiers are doing better than random guessing. Because, if the algorithms are complementary, then when one or a few algorithm makes an error, the probability is high that the remaining algorithms can correct this error. The main steps involved in the proposed system are depicted in the flowchart (Figure 2), that present a compact summary of our approach. The extensive tests have shown that combining the predictions of multiple detectors is more accurate than any of the individual detectors making up the ensemble.

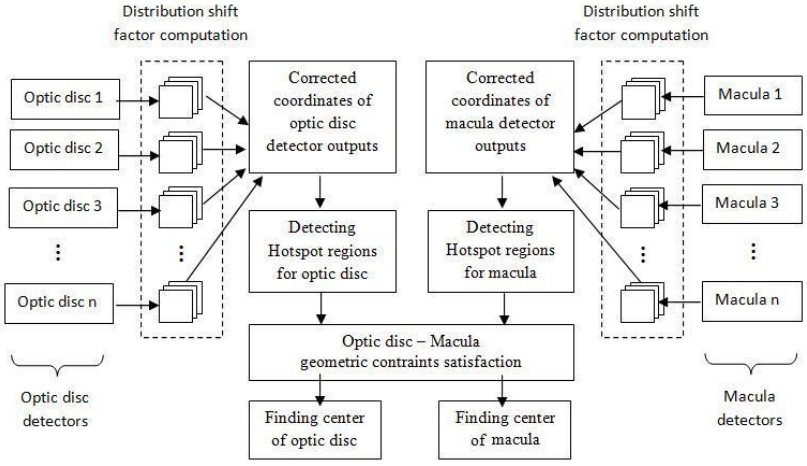

Fig. 2. Flowchart showing the steps of the proposed technique.

3.1 Computing distribution shift factors

The macula/OD centers detected by a particular algorithm in all test images are mapped onto a single image to check the distortion of its distribution. We observed that, the outputs generated by the algorithms are quite dispersed and deviated from the manually selected macula center. In Figure 3a, the Gaussian kernel density estimation of the M_I [17] algorithm outputs is shown for the macula and of the OD_{fv} [15] algorithm for the OD, respectively. Therefore, we propose to compute the distortion in the data and applying a shift operation prior to actual combination of outputs for finding macula center to make the individual algorithms unbiased. To compute the shift factor we calculate the average difference between the candidate of the algorithm and the manually selected macula center for those *n* images, where the algorithm successfully found the macula/OD region. That is, for the horizontal and vertical components of the shifting vector we have:

$$dx = \sum_{i=1}^{n} (x_i - x_{mi}) / n \quad , \quad dy = \sum_{i=1}^{n} (y_i - y_{mi}) / n \,,$$

where (x_i, y_i) stands for the fovea/OD center candidate of the algorithm on the i^{th} image, while (x_{mi}, y_{mi}) is for the manually selected fovea/OD center. The new outputs distribution is generated by applying the distortion shift factor on each output pixel coordinate. The improvement in the result can be seen in Figure 3.

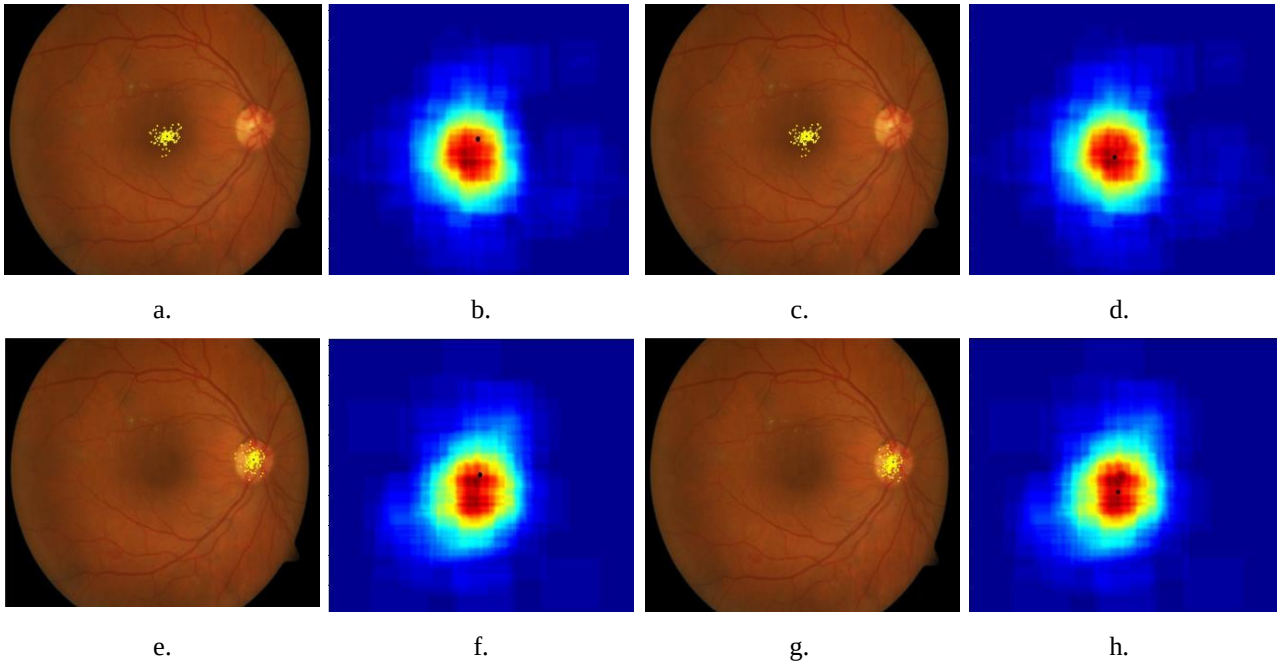

Fig. 3. a-d) The distortion in macula detector outputs[17] before and after applying shift factor, e-h) the distortion in OD algorithm [15] outputs before and after applying shift factor.

3.2 Detecting hotspot region for OD/macula

3.2.1 OD and macula detection separately

We first devised a circular template voting scheme to determine the hotspot region i.e., an area in the image where majority of the outputs lies. A circular template of radius R is fit on each pixel in the image and outputs of candidate algorithms that fall within the radius of the predefined circular template are counted. The circular template covering the maximum number of optic disc detector outputs in its radius is considered to be a hot spot. There can be more hot spots covering the maximum number of detector outputs in their radius; hence they together define a hot spot region, the patch with highest probability. The radius R of the template was set to 102 pixels, keeping in view the fact that clinically this is the average OD radius at the investigated resolution (field of view FOV equal to 1432). A circular template voting scheme has an intuitive appeal, and our results shows it works well in practice. Over all, we have used the outputs of the five algorithms for OD detection and five algorithms for macula detection, as discussed in section 2, in our combined system. Following the principal of majority voting, the center of the circular templates covering the maximum number of OD detectors and macula detector outputs in its radius is considered to be the OD and macula hotspots, respectively. If there is a tie then such conflict are handled using an additional post processing e.g., for OD detection, the Gaussian filter is applied on the green channel of the image with a large sigma ($\sigma = 300$). The smoothened image is then subtracted from the original image to get resultant image, a rather darker image in which OD appears as a brighter patch as compare to the background image. The average intensity around the detectors outputs is computed using the same circular template, and the template with the highest average intensity is selected as the best OD hotspot region.

In case of macula detection, we observed and tested that the vessel based macula detection algorithm M_{ta} [19] influenced the combination result therefore whenever there is conflicting situation or ties among hotspot regions, the

hotspot region containing algorithm M_{ta} output is given preference and is selected for further processing. If the output of M_{ta} is lying isolated and not as part of any hotspot regions detected, then such conflicting situation is handled by computing distance between hotspots centers and the center of the image followed by selecting the minimum distanced region.
Sometimes, majority voting may fail to detect the correct OD or macula center, especially in case of diseased retina (see figure 4, where template with three outputs is assumed to be the best hotspot for OD).

Fig. 4. False positive reported in the majority voting during OD detection.

Therefore, we proposed a more sophisticated alternative method to avoid these shortcomings, explained in the following section.

3.2.2 OD and macula detection based on mutual information

The raise in accuracy can be obtained by exploiting the anatomical constraints between OD and macula, particularly the information about distance and angle criteria can be used to choose the best candidate hotspot region pair. The minimum radius bounding circle around a set of points is a simple measure of the area they occupy, as well as a useful tool in graphical applications. Welzl [21] proposed a simple randomized algorithm for the minimum covering circle problem that runs in expected $O(N)$ time. Therefore to reduce the image processing needs instead of scanning the whole image, a minimum radius bounding is used to locate the hotspot region as being candidate of optic disc/macula. For this purpose, an un-ordered collection of different OD detectors and macula detectors are produced separately using combination rule:

$$C(n,r) = \frac{n!}{r!(n-r)!}$$

where n, r are non negative integers and $r \leq n$. Here, n is the number of detectors and r is the number of items taken from n elements. The minimal enclosing circle algorithm considers every circle defined by these set of detectors generated using combination without replacement. The algorithm returns center and radius of the circle defined by detectors. There can be many such circular regions, however to validate a region as being hotspot region (candidate for OD/macula), the OD radius is used as threshold criteria to accept or discard a circle. i.e., if the radius of the minimal enclosing circle is less than or equal to the OD radius, then such a circle is considered as candidate for OD/macula. For all hotspots regions for macula and optic disc detected in this way, we calculate the score using their mutual information and the candidate hotspot pair with maximum score is selected as the best hotspot region for macula and OD. The score of a pair is based on the cardinalities i.e., number of output present in a hotspot and penalties in term of distance and angle errors:

$$Score(M_i, OD_j) = |M_i| \times |OD_j| - \frac{D_{err}}{D_{avg}} - \frac{A_{err}}{A_{avg}} \quad .$$

Here, M_i is the i^{th} macular candidate hotspot and OD_j is the j^{th} OD candidate hotspot region, | . | stands for the cardinality of a set. D_{err} and A_{err} is the distance and angle error respectively, obtained as a difference between computed values and average values. Using manually marked macula and OD centers, we found that the average distance (D_{avg}) is 114 pixels and the average angle (A_{avg}) is ± 6º. Fig 5a shows the hotspot regions, the solid circles with triangles representing macula detectors and dashed circles with squares representing OD detectors are the macula and OD hotspots respectively. In Figure 5b, all possible OD/macula pairs are shown (dashed lines), the solid line between OD_1 and M_1 has the maximum score i.e., best satisfying the cardinality, distance and angle criteria.

3.3 Center of the Hotspot based on a weighted combination

The center of the final hotspot regions could be found by averaging algorithms outputs, however, for a more accurate estimation, weights can be associated with detector outputs to determine the final location. The principal difficulty is how to choose the 'right' weights. By following classical statistical recommendations, we assumed the observed data set to be linear combinations on certain basis. Therefore, weights w_i can be computed for the x-coordinates and y-coordinates of the detectors outputs.

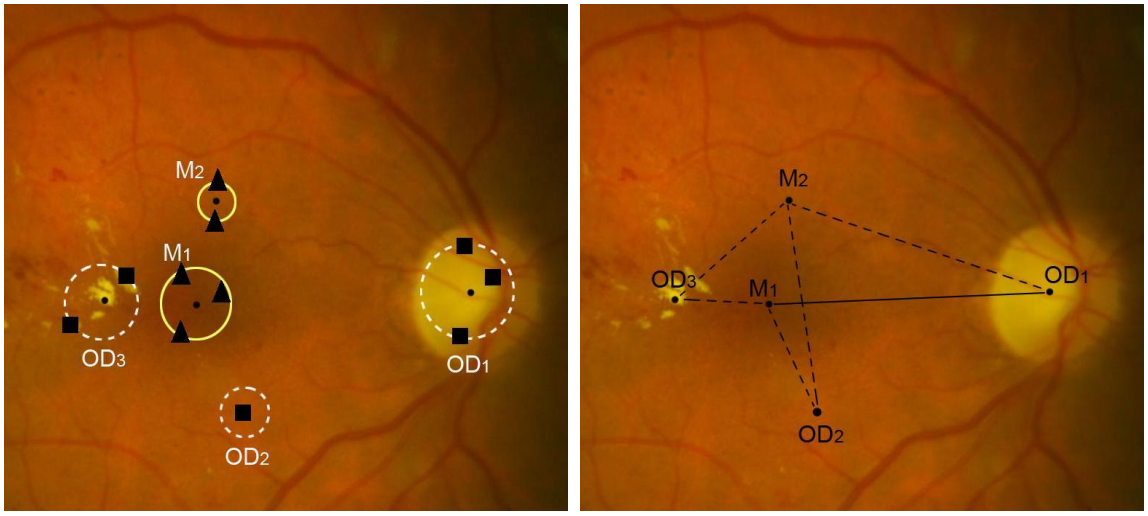

a. b.

Fig. 5 a) A retinal image with spotted hotspot regions for macula and OD, b) M_1 and OD_1 satisfying geometric constraints with highest score.

If we denote the output centers of the individual algorithms by random variables $S_1(x_1, y_1)$, $S_2(x_2, y_2)$, . . . , $S_N(x_N, y_N)$ with distinct variances $Var(S_i) = \sigma_i^2 > 0$, then the problem of outputs combination is to reduce these N outputs to one final center $S_w(x_w, y_w)$. An appropriate combination of the outputs can be the weighted linear combination

$$S_w = \sum_{i=1}^{N} w_i S_i \quad , \qquad (1)$$

where w_1, w_2, . . . , w_N are non-negative weights, constrained to sum to 1. This constraint guarantees the combined estimate to remain unbiased. The variance of the estimator S_w is determined by the choice of weights and the variances of the individual outputs. When the random variables are independent then the variance of the estimator S_w is determined only by the choice of weights and the variance of individual outputs. In this case we have to minimize the expression below

$$Var(S_w) = \sum_{i=1}^{n} w_i^2 \, Var(S_i) \quad . \qquad (2)$$

In this way the choice of weights that minimize the variance of the combined estimate is

$$w_i = \sigma_i^{-2} \Big/ \sum_{j=1}^{n} \sigma_j^{-2}$$

as a result of [22]. Choosing these weights leads to small variance, hence, the expected Euclidean distance from the true center of the combined estimate can be minimized. The higher the weight for an output, the more that detector is trusted to provide the correct answer. In the other case, when the random variables are dependent then we have to consider the pair wise covariances, as well. We minimize

$$Var(S_w) = \sum_{i=1}^{N} w_i^2 \, Var(S_i) + 2 \sum_{1 \le i < j \le N} w_i w_j \, Cov(S_i, S_j) \quad (3)$$

to get the optimal combinations for the weights. We can also write (3) as $Var(S_w) = \mathbf{w}^T \boldsymbol{D} \, \mathbf{w}$, where $\mathbf{w}$ is a vector containing the weights and $\boldsymbol{D}$ is a matrix containing the pair-wise covariances. This minimum problem can be solved via derivation i.e., $(\partial Var(S_w) / \partial w_i = 0)$ should be solved for the N variables $w_1, w_2, \ldots, w_N$ to determine the proper weights.

In our setup, we have compared all the macula and OD detectors, respectively with χ^2 – test to check their independency. Then, according to above description we removed the term $Cov(S_i, S_j)$ from (3), when the i^{th} and j^{th} algorithms were proven to be independent.

IV. RESULTS AND DISCUSSION

We have evaluated our proposed combination of algorithms to localize optic disc and macula on the publically available three benchmark listed in Table. 1.

TABLE I.
THE TRAINING AND TEST DATABASES USED

Benchmark	Resolution	No. of images
Diaretdb0 [9]	1500×1152	130
Diaretdb1[10]	1500×1152	89
DRIVE [11]	565×584, 730×490	40

The proposed algorithm should be trained on the training database (without influence of the test database). Therefore, the set of images from the three benchmarks listed in Table. 1 has been split into a training database and a test database. The training database contains 40% of the images from each benchmark and the test database contains the rest of 60% of the images. To reduce variability, multiple rounds of cross-validation are performed using different partitions, performing the analysis on one subset (the training set), and validating the analysis on the other subset (the validation set or testing set).

4.1 Optic disc detection results

The methods have been evaluated on the basis of two criterions i.e., to fall inside the manually selected optic disc patches (see Figure 6), and to be close to the manually selected OD center. Table 2 shows the correct detection of the OD location based on optic disc patch; the percentage detection rate of the proposed approach is higher than any of the individual algorithms. In Table 3 we can see the secondary error term that measures the average Euclidean distance of the candidates from the manually selected OD centers. We can observe that the combined system led to more accurate center localization than any of the individual algorithms.

Fig. 6. A retinal image with manually selected optic disc patch

TABLE II. CANDIDATES FALLING INSIDE MANUALLY SELECTED OD PATCH.

	Optic Disc detector algorithms					
Test databases	OD_{pd}	OD_{ed}	OD_{fv}	OD_{ef}	OD_{ht}	**Combined system**
Diaretdb0	89.52 %	77.56 %	78.20 %	95.29 %	80.12 %	96.79 %
Diaretdb1	88.99 %	75.46 %	77.04 %	93.70 %	76.41 %	94.02 %
Drive	80.55 %	97.22 %	67.35 %	98.61 %	86.10 %	100 %
Total average	87.95 %	79.88 %	76.12 %	95.26 %	79.78 %	96.34 %

Table III. average Euclidean error of the OD candidates

	Optic Disc detector algorithms					
Test databases	OD_{pd}	OD_{ed}	OD_{fv}	OD_{ef}	OD_{ht}	**Combined system**
Diaretdb0	15.89	20.63	18.55	11.89	11.41	12.23
Diaretdb1	17.38	20.84	20.41	13.05	11.95	11.95
Drive	23.31	13.21	20.69	16.98	14.67	15.95
Total average	17.54	19.55	19.52	13.07	12.10	12.71

4.2 Macula detection results

To localize macula and detect fovea, we tested the five algorithms listed in section 2 on the same three databases of Table 1. The methods have been evaluated on the basis of two criterions i.e., macula error and fovea error. The macula error is the number of times the algorithm's output falls within the 0.5 DD radius of the manually selected macula center (Table 4), and fovea error i.e., the average Euclidean distance of these candidates and the manually selected centers (see Table 5). Results are given in pixels at the resolution of ROI diameter = 1432 (average ROI diameter of Diaretdb0 and Diaretdb01). Weights are calculated with considering the algorithms dependencies. Just like the OD, the combined system provided more accurate results than any of the individual algorithms both for the primary error and secondary error terms,

TABLE IV
CANDIDATES FALLING IN MACULA REGION.

	Fovea detector algorithms					
Test databases	M_I	M_{sr}	M_{ta}	M_n	M_{wm}	**Combined system**
Diaretdb0	67.94 %	70.29 %	82.47 %	86.10 %	60.67 %	93.58 %
Diaretdb1	60.373 %	77.66 %	78.29 %	91.50 %	71.69 %	99.68 %
Drive	72.06 %	81.07 %	58.55 %	81.07 %	81.07 %	91.88 %
Total average	65.77 %	74.24 %	78.03 %	87.39 %	67.10 %	95.53 %

TABLE V.
AVERAGE EUCLIDEAN ERROR OF THE FOVEA CANDIDATES.

	Fovea detector algorithms					
Test databases	M_I	M_{sr}	M_{ta}	M_n	M_{wm}	**Combined system**
Diaretdb0	29.98	31.63	52.13	35.57	29.28	29.64
Diaretdb1	27.05	29.93	47.88	28.86	27.75	24.26
Drive	16.52	24.19	61.68	36.08	22.19	26.80
Total average	27.27	30.11	51.81	33.25	27.86	27.38

4.3 Joint OD-macula detection results

Research in ensemble methods has largely revolved around designing ensembles consisting of competent yet complementary models. The goal of the proposed approach is to leverage the power of multiple OD and macula detector that are competent but also complementary. The results demonstrate that the use of mutual geometric constraints between OD and macula has improved upon traditional approaches like simple averaging or voting. Weighted averaging has proven to be very effective and has achieved better prediction accuracy than any of the individual algorithm could have on their own (Figure 6). The use of geometric constraints between OD and macula

is a unique contribution which has been rewarded as it outperforms all individual decisions and separate combination as shown in Table 6. Therefore, practitioners in diabetic retinopathy should stay tuned for further developments in the vibrant area of multiple algorithm based decision making.

TABLE VI
OD / MACULA DETECTION BASED ON MUTUAL INFORMATION.

	Joint OD-macula detection	
Test databases	***Macula***	***OD***
Diaretdb0	96.79	97.64
Diaretdb1	98.74	97.79
Drive	91.73	100
Total average	**96.87**	**98.06**

V. CONCLUSION

We developed a framework for combining state-of-the-art OD/fovea detector in a flexible way. The aim was to give an intuitive understanding of the potential advantage of ensemble methods in term of improving performance as compared to individual algorithms. We showed that our combination outperformed all the individual algorithms. We have used a majority voting and weighted linear combination based scheme that count the number of outputs of the algorithms falling in a specified radius circle, and is marked as a hotspot. Our method achieved highest performance, and closest to the manually selected optic disc center chosen by a retinal specialist. This proposed combination is just one possibility; there is still room for further improvement through further research by combining other methods. We tried to check the influence of each algorithm present in our combination system by excluding it and running the test again with rest of algorithm. In both cases i.e., OD and macula we found that all the algorithms were potentially useful and excluding any of them did not improve the results rather it decrease the detection rate.

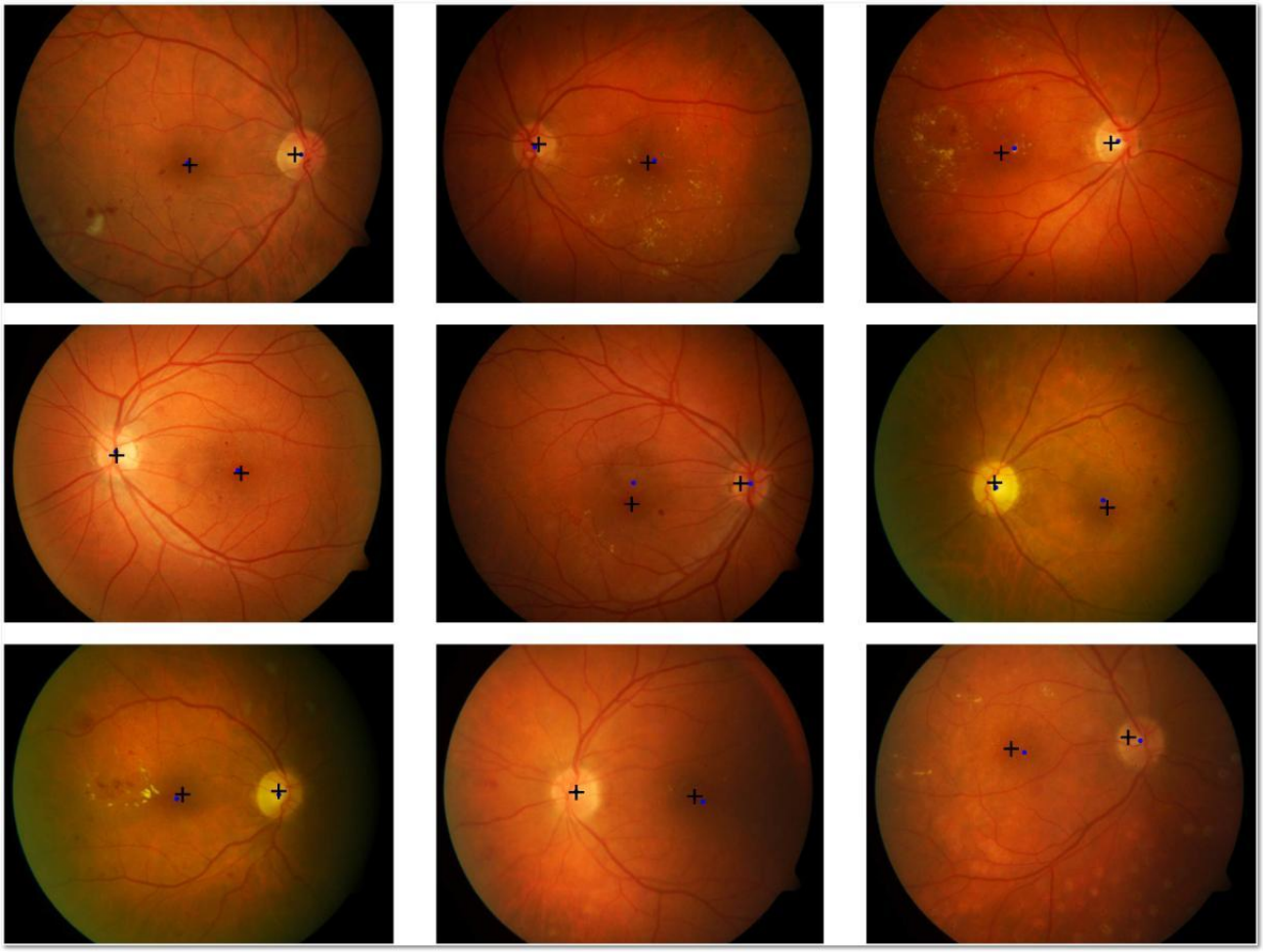

Fig. 6. Joint macula-OD detection results, the plus signs indicates system outpus against dots (the manually choosen by opthamologist)

ACKNOWLEDGMENT

This work was supported in part by the Janos Bolyai grant of the Hungarian Academy of Sciences, by the TECH08-2 project DRSCREEN- Developing a computer based image processing system for diabetic retinopathy screening of the National Office for Research and Technology of Hungary (contract no.: OM-00194/2008, OM-00195/2008, OM-00196/2008), and by the NIHR BMRC for Ophthalmology.

REFERENCES

[1] C. Sinthanayothin, J. F. Boyce, T. H. Williamson, H. L. Cook, E. Mensah, S. Lal, and D. Usher, Automated Detection of Diabetic Retinopathy on Digital Fundus Images, Diabetic Medicine. 19(2002), 105–112.

[2] M. Niemeijer, M. D. Abràmoff, and B. van Ginneken, Segmentation of the Optic Disc, Macula and Vascular Arch in Fundus Photographs, IEEE trans. on medical imaging. 26(2007), 116–127.

[3] Lalonde, M., Beaulieu, M. and Gagnon, L., Fast and Robust Optic Disk Detection using Pyramidal Decomposition and Hausdorff-Based Template Matching, IEEE Trans. Medical Imaging. 20(2001), 1193-1200.

[4] Sopharak, A., Thet New, K., Aye Moe, Y., N. Dailey, M., Uyyanonvara, B., Automatic Exudate Detection with a Naive Bayes Classifier, International Conference on Embedded Systems and Intelligent Technology, Bangkok, Thailand, 2008, pp. 139–142.

[5] A. Hoover and M. Goldbaum, Locating the Optic Nerve in a Retinal Image using the Fuzzy Convergence of the Blood Vessels, IEEE Trans. Med. Imag. 22(2003), 951-958.

[6] F. Mendels, C. Heneghan, and J. P. Thiran, Identification of the Optic Disk Boundary in Retinal Images using Active Contours, in Proc. Irish Machine Vision Image Processing Conf, 1999, pp. 103–115.

[7] S. Sekhar, W. Al-Nuaimy, and A. Nandi, Automated Localisation of Retinal Optic Disk using Hough Transform, in Proceedings of the 5th IEEE International Symposium on Biomedical Imaging: From Nano to Macro, ISBI 2008, Paris, 2008, pp. 1577–1580.

[8] Abramoff, M. D., Niemeijer, M., The Automatic Detection of the Optic Disc Location in Retinal Images using Optic Disc Location Regression, In 28th Annual International Conference of the IEEE Engineering in Medicine and Biology Society, 2006, pp. 4432–4435.

[9] T. Kauppi, V. Kalesnykiene, J.K. Kamarainen, L. Lensu, I. Sorri, H. Uusitalo, H. Kalviainen, J. Pietila, Diaretdb0: Evaluation database and methodology for diabetic retinopathy algorithms, *Technical report*, Lappeenranta University of Technology, Lappeenranta, Finland, 2006.

[10] T. Kauppi, V. Kalesnykiene, J.K. Kamarainen, L. Lensu, I. Sorri, A. Raninen, R. Voutilainen, J. Pietilä, H. Kälviäinen, H. Uusitalo, Diaretdb1 diabetic retinopathy database and evaluation protocol, In Proc. of the Medical Image Understanding and Analysis, Aberystwyth, UK, 2007, pp. 61–65.

[11] J. J. Staal, M. D. Abramoff, M. Niemeijer, M. A. Viergever, and B. van Ginneken, Ridge Based Vessel Segmentation in Color Images of the Retina, IEEE Transactions on Medical Imaging. 23(2004), 501–509.

[12] Dietterich T. G., Ensemble Methods in Machine Learning, Multiple Classifier Systems, LNCS. 1857(2008), 1-15.

[13] N. Otsu, A Threshold Selection Method from Gray-Level Histograms, IEEE Trans. Syst. Man and Cybern. 1979, pp. 62-66.

[14] S. Ravishankar, A. Jain, A. Mittal, Automated Feature Extraction for Early Detection of Diabetic Retinopathy in Fundus Images, IEEE Conference on Computer Vision and Pattern Recognition, 2009, pp. 210-217.

[15] M. Niemeijer, M. D. Abràmoff , B. van Ginneken, Fast detection of the optic disc and fovea in color fundus photographs, Medical Image Analysis. 13(2009), 859–870.

[16] M. Niemeijer, J.J. Staal, B. van Ginneken, M. Loog, M.D. Abramoff, Comparative study of retinal vessel segmentation methods on a new publicly available database, in: SPIE Medical Imaging. 5370(2004), 648-656.

[17] T. Petsatodis, A. Diamantis, G.P. Syrcos, A Complete Algorithm for Automatic Human Recognition based on Retina Vascular Network Characteristics, 1st International Scientific Conference e RA, Tripolis, Greece, 2004, pp. 41- 46.

[18] S. Sekhar, W. Al-Nuaimy, A. K. Nandi, Automated localization of optic disc and fovea in retinal fundus images, 16th European Signal Processing Conference, Lausanne, Switzerland, 2008.

[19] A. D. Fleming, S. Philip, K. A. Goatman, J. A. Olson, and P.F. Sharp, Automated Assessment of Diabetic Retinal Image Quality Based on Clarity and Field Definition, Investigative Ophthalmology and Visual Science. 47(2006), 1120-1125.

[20] F. Zana, I. Meunier , J. C. Klein, A region merging algorithm using mathematical morphology: application to macula detection, Proceedings of the fourth international symposium on Mathematical morphology and its applications to image and signal processing, Amsterdam, The Netherlands, 1998, pp. 423 - 430.

[21] E. Welzl, Smallest Enclosing Disks (Balls and Ellipsoids), New Results and New Trends in Computer Science, LNCS. 555(1991), 359–37.

[22] W. G. Cochran, Problems arising in the analysis of a series of similar experiments, J. of the Royal Statistical Society. 4(1937), 102–118.

Correspondence to: Dr. Andras Hajdu
Faculty of Informatics, University of Debrecen, 4010 Debrecen, POB 12, Hungary
Phone: +36-52-512900/62830
Fax: +36-52-416857
E-mail: hajdu.andras@inf.unideb.hu